Journal of volcanology
and geothermal research

Modeling Strombolian eruptions of Karymsky volcano, Kamchatka, Russia

A. Ozerov [a], I. Ispolatov [b,c,*], J. Lees [d]

[a] *Institute of Volcanology, Russian Academy of Science, Petropavlovsk-Kamchatsky 683006, Russia*
[b] *Departamento de Fisica, Universidad de Santiago de Chile, Av. Equador 3493, Santiago, Chile*
[c] *Department of Chemistry, Cornell University, Ithaca, NY 14853, USA*
[d] *Department of Geological Sciences, University of North Carolina, Chapel Hill, NC 27599-3315, USA*

Abstract

A model is proposed to explain temporal patterns of activity in a class of periodically exploding Strombolian-type andesite volcanoes. These patterns include major events (explosions) which occur every 3–30 min and subsequent tremor with a typical period of 1 s. This two-periodic activity is thought to be caused by two distinct mechanisms of accumulation of the elastic energy in the moving magma column: compressibility of the magma in the conduit and viscoelastic response of the almost solid magma plug on the top. A release of the elastic energy occurs during a stick–slip dynamic phase transition in a boundary layer along the walls of the conduit; this phase transition is driven by the shear stress accumulated in the boundary layer. The intrinsic hysteresis of this first-order phase transition explains the long periods of inactivity in the explosion cycle. Temporal characteristics of the model are found to be qualitatively similar to the acoustic and seismic signals recorded at Karymsky volcano in Kamchatka.
© 2003 Elsevier Science B.V. All rights reserved.

1. Introduction

A wide variety of types of volcanic activity exists: from devastating explosions separated by calm periods of many years or even centuries to a steady continuous outpouring of magma. In this paper we study mechanisms that give rise to a Strombolian-type volcanic activity, which is some-

where between these two extremes. The Strombolian-type activity is common for volcanoes with viscous andesite magmas and is characterized by regularly repeated explosions (10–400 per day) followed by relatively calm periods. Often in the course of a longer explosion, the gas and ash emission exhibits audible and visible modulations with a rather robust period of about 1 s. These modulations, often found on the seismograms of Strombolian-type eruptions (see, for example, Chouet et al., 1999), received a special name, 'chugging' (Benoit and McNutt, 1997), because they resemble a periodic noise produced by a steam engine. An example of a volcano exhibiting

* Corresponding author. Tel.: +56-2776-3322, ext. 212; Fax: +56-2-776-9596.
  E-mail address: jaros007@hotmail.com (I. Ispolatov).

such activity, we consider Karymsky volcano on Kamchatka peninsula in the far east of Russia.

We believe that these Strombolian-type eruption patterns are caused by peculiarities of the motion of the magma column and propose model that describes the magma motion in a volcanic conduit as a creep flow of viscoelastic compressible medium with shear-stress-dependent boundary conditions. We show that the dynamics of the model indeed exhibits two levels of quasiperiodic behavior and resembles the eruption patterns of the Strombolian-type volcanoes both on long and short timescales. The physical transparency of the suggested model allows us to derive equations expressing the typical eruption timescales through the material properties of the magma and geometrical characteristic of the conduit.

Our paper is organized in the following way: first, we briefly describe geological aspects and seismo-acoustic observations of the most recent
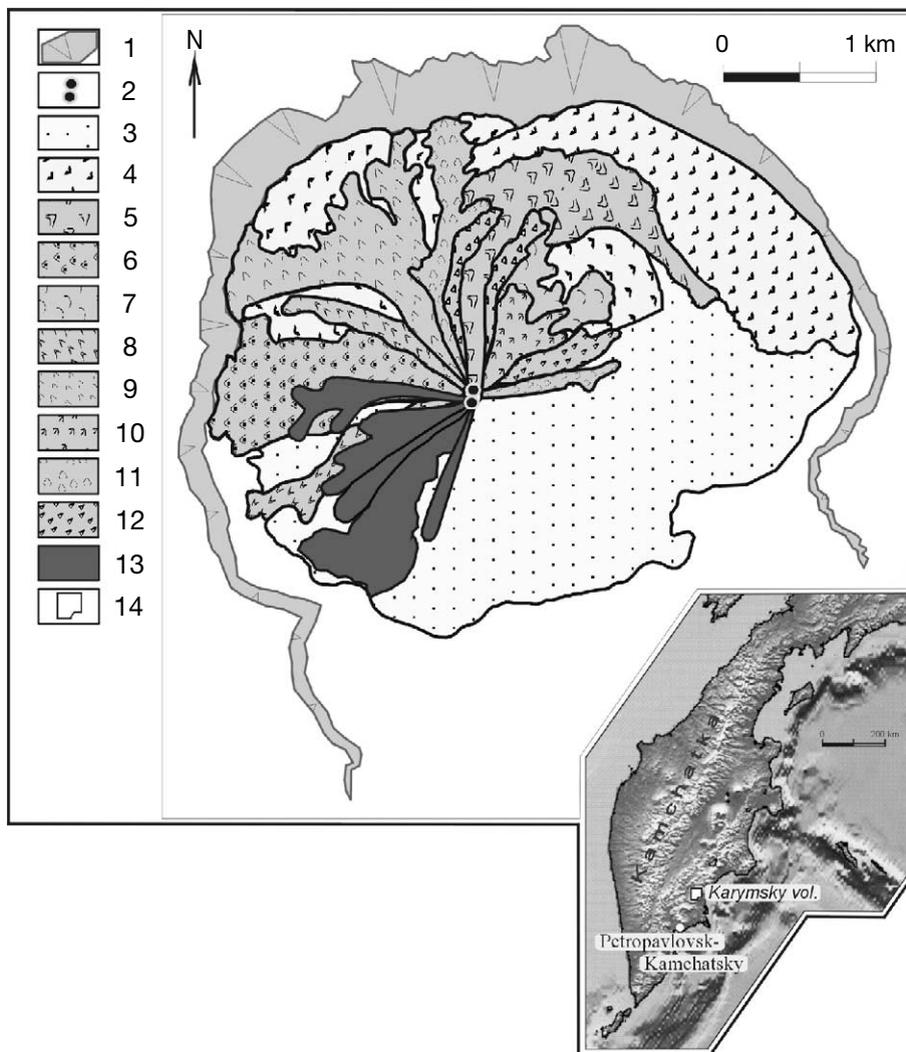

Fig. 1. Map of Karymsky volcano according to Hrenov et al. (1982) with the additions of the authors. 1. Karymsky caldera. 2. Summit double crater. 3. Modern loose deposits on the cone. 4–13. Lava flows by dates: 4. 1600?–1800?; 5. 1908?–1935?; 6. 1963–1965; 7. 1970; 8. 1971; 9. 1976; 10. 1978; 11. 1979; 12. 1980; 13. 1996–2000. 14. Location of the insert on the map of Kamchatka peninsula.

eruption of Karymsky volcano (1996–2000). Then, after referring to the existing explanations of Strombolian-type activity, the model is formally introduced. We derive simple analytical expressions for a dormant time, a duration of explosion, and a typical period of tremor, and then present a numerical solution to a system of dynamical equations describing the motion of the magma column. The paper is concluded with a discussion of results and possible directions for further studies.

2. The Karymsky eruption of 1996–2000

Karymsky volcano (Figs. 1–3), located in the

Fig. 2. The summit of Karymsky volcano during the 1996–2000 eruption. Bombs and ash are ejected from the southern (the front) part of the crater. The lava flows from a clearly visible effusive bocca, located 80 m below the crater. The photo is taken during a longer explosion when a higher-intensity initial stage is followed by tens of seconds of a lower-intensity ash and steam ejection. Photo by A. Ozerov.

Fig. 3. A powerful explosive eruption from the summit crater of Karymsky volcano, September 9, 1998, view from the west. The height of eruptive column is ∼500 m. The traces of rolling volcanic bombs are clearly visible on the slopes of the volcano. Photo by A. Ozerov.

central part of the East Kamchatka volcanic belt, is one of the most active volcanoes in far-eastern Russia. It is a typical andesite stratovolcano composed of a 7700–7800-year-old caldera ∼5 km in diameter (Hrenov et al., 1982) and a more recent cone which started growing in the central part of the caldera about 5300 years ago and at present (September 2000) is ∼700 m high. The cone is composed of accumulated lava and pyroclastic materials; the elevation of the summit is 1549 m above sea level. The most recent Karymsky eruption began in January 1996 and entered a lull phase in December 2000; the previous eruption lasted from 1970 to 1982 (Ozerov, 1997; Fedotov et al., 2001). Generally, Karymsky activity can be characterized as effusive–explosive: each eruption consisted mostly of discrete quasiperiodic gas and ash bursts which sent plumes 100–1000 m above the crater rim (Figs. 2 and 3). In the lower part of the eruption column, hot volcanic bombs up to 2 m (rarely up to 5 m) in size were frequently observed. The bombs were dense, angular, and had shell-like fracture. On the surface of some bombs, noticeable extrusive tracks were found; they were scratched on the very viscous moving magma by the protruding parts of the magma channel. Ash

and steam clouds have been observed extending downwind for 10–50 km, rarely 100–200 km. During particularly strong explosions, the eruption column collapsed causing pyroclastic flows. An active part of the crater (Fig. 2), formed during the 1996–2000 eruption, widened from 90 m in 1996 to 190 m in 2000, A lava flow field, produced by the very viscous magma, runs down the southwestern slope of the cone and reaches a length of ∼1.4 km and width of ∼100–200 m (Fig. 3). Even during the periods of highest activity, the advancement of the lava flows was very slow (few meters per day).

From the aerophotogrammetry and ash collection data, the total volumes of pyroclastic and effusive materials deposited on the cone of Karymsky during the eruption of 1996–2000 are estimated to be 0.0274 and 0.0229 km^3, respectively (Fedotov et al., 2001). Eruptive products, which include lava, volcanic bombs, and ash, predominantly consist of andesite, usually of black and dark gray color. Plagioclase (up to 3–5 mm) is the most abundant phenocryst phase (20–25%), pyroxene and olivine (2–3 mm) are generally subordinate (less than 1%). A major oxide composition averaged over six samples from the 1996–

2000 eruption is listed below (weight percent): SiO_2 – 61.54, TiO_2 – 0.86, Al_2O_3 – 16.67, Fe_2O_3 – 2.43, FeO – 5.12, MnO – 0.11, MgO – 1.99, CaO – 5.31, Na_2O – 3.69, K_2O – 1.58, P_2O_5 – 0.25.

The feeding system of Karymsky volcano was studied by various methods, including gravity surveys, aeromagnetic surveys, photogrammetry, seismology and geodesy (Zubin et al., 1971; Magus'kin et al., 1982; Shirokov et al., 1988). Despite slight discrepancies in the estimates of the depth of the upper border of the magma chamber and its size, these data agree that underneath the Karymsky volcano in the close proximity to the surface there exists a magma chamber. The upper border of this chamber is a few kilometers below sea level. The diameter of the magma chamber is estimated to be between 1.5 and 7 km. A magma channel of a diameter of 100–200 m leads from the magma chamber to the summit crater.

3. Dual periodicity of the Karymsky eruption

A distinctive feature of Karymsky eruptions is its rather robust periodicity which is observed on two timescales. An explosion, and a following quiet period, define the first period of activity which varied between 3 and 30 min and sometimes extended up to 1 h. An explosion itself can start either abruptly or gradually (Fig. 4) and proceed according to one of the following scenarios: during shorter explosions, the activity decays quickly and monotonously (in less than 10 s), while the longer explosions (20–40 s, rarely 1 min) may contain intervals of relatively high
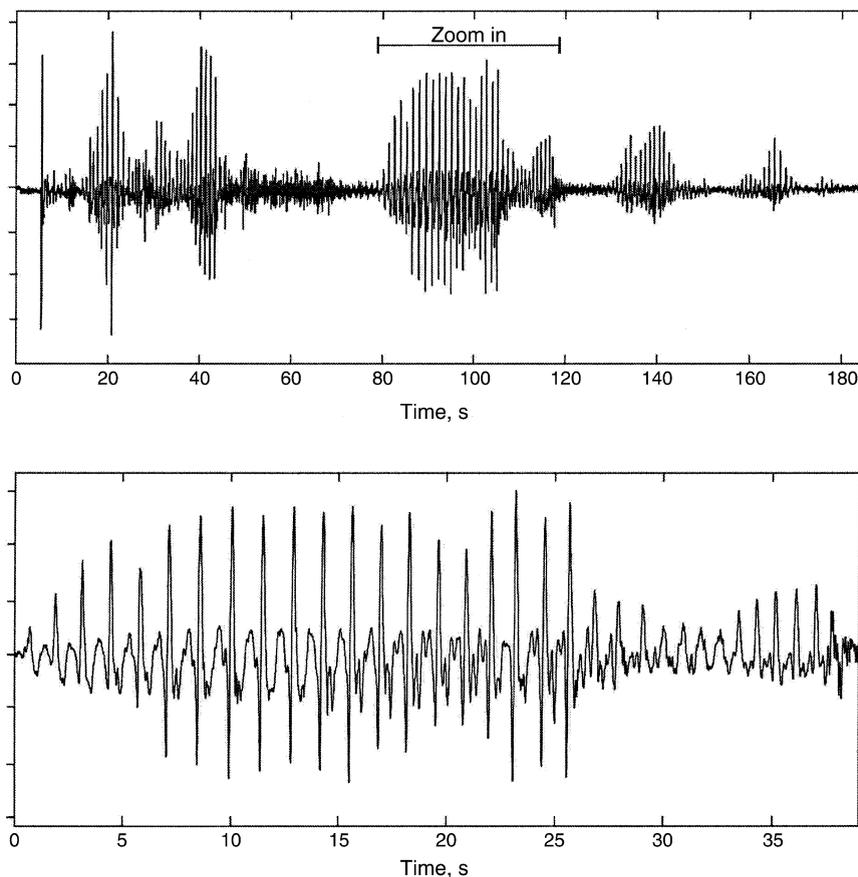

Fig. 4. Typical acoustic signal of a period of activity of Karymsky volcano.

and low activity. Often during longer (> 20s) explosions, the intensity of the acoustic and seismic signals emitted by the volcano exhibits chugging, i.e. modulations with a typical period of ∼1 s. The chugging defines the second, shorter period in the cyclic activity of the volcano. A typical chugging event consists of 10–20 cycles (Fig. 4). The explosion is followed by a quiet interval characterized by a complete lack of any activity in the crater and usually lasting much longer than the explosions themselves. Similar temporal patterns have also been observed during previous Karymsky eruptions. (Tokarev and Firstov, 1967; Farberov et al., 1983).

Detailed seismic and acoustic studies of Karymsky volcano were conducted in 1997–1999 by three Russian–US expeditions. The acoustic signals presented in Fig. 4 were recorded on August 21, 1997 using a set of infrasound microphones. For a more complete description of the seismic and infrasound recordings at Karymsky the reader is referred to Johnson et al. (1998), Johnson (2000), and Johnson and Lees (2000).

4. Existing models of eruption periodicity

Currently there is no single well-established view of the mechanism that causes periodic patterns in Strombolian-type eruptions. Below we mention several possible explanations of origins of the periodicity. Lees and Bolton (1998) compared the eruption process to steam exhaust from a hydrodynamic system with a non-linearly controlled exhaust valve resembling a pressure cooker. Manga (1996) suggested that the periodicity is caused by the segregation of ascending bubbles into waves, as in a pint of Guinness beer. Julian (1994) proposed a mechanism of non-linear hydrodynamic oscillations in the ascending magma flow. Jaupart and Vergniolle (1989) suggested that oscillations are caused by periodic collapse of a bubble foam trapped in pockets of the magma chamber. Recently, there appeared a paper by Denlinger and Hoblitt (1999) where an ad hoc hysteresis model was developed to describe the periodic behavior of silicic volcanoes. However, a self-consistent explanation for both long- and

short-time periodicity with extended calm periods exemplified in the activity of Strombolian-type volcanoes is still missing. Our model, based on a viscoelastic hydrodynamical description of the motion of the magma column with shear-stress-dependent boundary conditions, accounts for both timescales.

5. The model

Let us first qualitatively discuss the motion of magma in the conduit. Since the temperature and pressure in the magma column decrease with the height, the viscosity of magma increases rapidly in the upper part of the conduit. Inspecting eruption products ejected onto the surface, it is natural to deduce that at the very top of the column the magma is almost solid. However, deeper parts of the magma column are still hot and much less viscous. Given this significant difference in rheological properties of the upper and lower sections of the magma column, we introduce the following idealization: the moving magma is considered as consisting of two distinct uniform parts: long lower part (LP) and short upper part (UP). To simplify the model even further, we assume that the viscosity of the magma in the LP is negligible compared to the viscosity of the UP. If necessary, the viscosity of the LP can be approximately taken into account by increasing the effective viscosity of the UP. We also assume that there is a constant supply of fresh magma to the bottom of the LP. Unlike the LP, magma in the UP is cold and viscous; in addition, as any media near the liquid–solid transition point, it possesses a certain degree of elasticity. Because of the small length (and therefore, volume) of the UP compared to the LP (∼100 m vs. ∼5 km), the relative contribution of the UP to the compression of the whole magma column is minor and can be neglected. In summary, we consider a long cylindrical tube filled with a non-viscous compressible media, fed at the bottom with a constant velocity and a short viscoelastic plug (UP) on the top. As the viscosity of the LP is assumed to negligible, the boundary conditions for the LP are irrelevant; the boundary conditions for the UP are controlled

by a local value of the shear stress in the vicinity of the cylinder wall. When the boundary shear stress is low, the plug 'sticks' to the cylinder wall and the boundary velocity is zero. As the shear stress increases, the magma near the wall undergoes phase transition (shear thins) to a much less viscous liquid state, and the boundary layer of the plug slips along the walls of the channel. This shear-induced phase transition happens when the viscoelastic state with the non-zero shear modulus becomes thermodynamically less stable than a pure liquid state with zero shear modulus. Phenomenologically, the transition between stick and slip boundary conditions for the very viscous body is similar to the effect of dry friction, where a motion begins only when a driving force exceeds some threshold value (Persson, 1999, chapter 8).

Qualitatively, a cycle of the system evolution can be described as follows: when the pressure in the compressible LP of the column is low, the shear stress σ in the plug is much smaller than the threshold phase transition value σ_{slip}, and the velocity of the UP is much less than the feeding velocity V_0. The difference in feeding and plug velocities results in the growth of the pressure of the compressible magma in LP which, in its turn, increases the shear stress in the plug. This stage corresponds to the dormant period between explosions. When the shear stress in the boundary layer of the UP exceeds the critical value σ_{slip}, the stick–slip phase transition occurs and the plug begins to move. This corresponds to the appearance of visible signs of a volcanic explosion.

Depending on the parameters of the model, the further evolution of the system proceeds according to one of the following two scenarios. For certain conditions, a relaxation of the viscoelastic deformation accumulated in the UP can result in a low, or even reverse, velocity of the boundary layer of the UP relative to the walls of the conduit. If these conditions persist for sufficient time, they can cause a drop of the shear stress below the slip–stick transition critical value σ_{stick}, which in turn can give rise to the reverse, slip–stick transition. However, the stick state will be very short-lived, since the accumulated excessive pressure in the LP and oscillatory motion of UP will result in

the immediate increase of the boundary shear stress and a new stick–slip transition. The length of a period of such coupled viscoelastic stick–slip process is controlled by the density, the elastic modulus, and the characteristic time of the phase transition. In the second scenario, sticking does not occur during short periodic viscoelastic oscillations of the UP, and the period of these oscillations is roughly equal to that of a freely oscillating elastic membrane with mixed boundary conditions. Either of these oscillation processes can cause the short-period modulation (~ 1 s) of the activity of the volcano.

During the active phase, the velocity of the UP is much higher than the feeding velocity V_0, which results in an expansion of the LP and a decrease of pressure under the UP. When the pressure under the UP drops so that the shear stress in the UP is below the slip–stick threshold value σ_{stick}, a 'long-term' sticking of the plug occurs, and the system enters a new quiet period. Because of the hysteresis ($\sigma_{stick} < \sigma_{slip}$) associated with the first-order nature of the stick–slip transition, it takes some time to build enough pressure for a new explosion to begin. This cycle corresponds to the second, longer period (3–30 min) in the dynamics of eruption.

Although simple in nature, this model is based on solid hydrodynamics and thermodynamics principles, qualitatively explains both scales of periodicity of Karymsky volcano and does not contradict the observations. Below a formal analysis of the dynamics of the model is presented.

Let us consider a cylinder (LP) of radius R and length L, filled with an ideal non-viscous compressible medium fed from the bottom with constant velocity V_0. The top of LP ends with a short viscoelastic plug (UP) of length l, $l \ll L$ (Fig. 5). The velocity field in the UP, of density ρ and driven by pressure P and stress tensor σ_{ij}, is described by the Navier–Stokes equation:

$$\rho \frac{\partial v_j}{\partial t} = -\frac{\partial P}{\partial x_j} + \frac{\partial \sigma_{ij}}{\partial x_i} \tag{1}$$

Because of the high viscosity and the low velocity of magma in the UP, the non-linear (convective) term is omitted. To account for the viscoelastic properties of the UP we use the simple
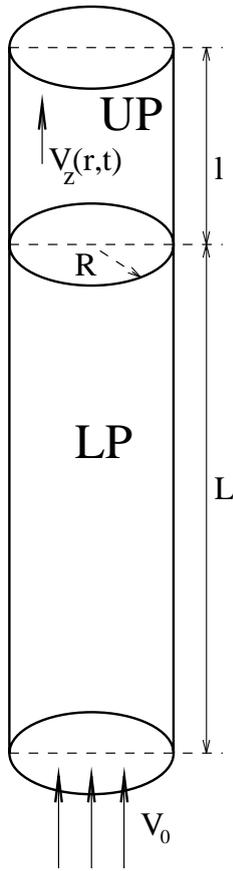
Fig. 5. Sketch of the magma conduit.

linear Maxwell model (see, for example, Bird et al., 1987), with a characteristic memory time τ_m:

$$\tau_m \frac{\partial \sigma_{ij}}{\partial t} = -\sigma_{ij} + \eta e_{ij} \qquad (2)$$

Here η is the dynamic viscosity, and $e_{ij} \equiv \partial v_i / \partial x_j + \partial v_j / \partial x_i$ is the shear rate tensor. Incompressibility condition for the magma in the UP reads:

$$\sum_{i=1}^{3} \frac{\partial v_i}{\partial x_i} = 0 \qquad (3)$$

For simplicity, we assume that the motion of the plug is axially symmetric and select the z direction of our cylindrical coordinate system parallel the axis of the cylinder directed along the magma flow. Also, we consider the pressure gradient constant through the UP and being equal to

$-P_0/l$, where P_0 is a pressure at the bottom of the UP. Using Eqs. 2 and 3, the Navier–Stokes equation (Eq. 1) can be transformed to:

$$\rho \frac{\partial V_z(r,t)}{\partial t} =$$

$$\frac{P_0(t)}{l} + \frac{\eta}{\tau_m} \int^t \exp\left(-\frac{t-t'}{\tau_m}\right) \Delta_r V_z(r,t') \, dt' \qquad (4)$$

Here V_z is the z component of the velocity of the plug averaged over the plug length, $\Delta_r \equiv \partial^2/\partial r^2 + (1/r)(\partial/\partial r)$ is the radial part of the Laplacian operator in cylindrical coordinates.

From the conservation of mass of the compressible media in the LP, it follows that the pressure P_0 on the bottom surface of the UP and the velocity of the UP are related as:

$$V(t) - V_0 =$$

$$-\beta L \frac{dP_0(t)}{dt}, \ V(t) \equiv 2 \int_0^R V_z(r,t) r \, dr / R^2 \qquad (5)$$

where $\beta \equiv -1/w(\partial w/\partial p)_T$ is the compressibility (isothermal) of the media in the LP (w is the volume), and $V(t)$ is the velocity of the UP $V_z(r,t)$, averaged over the radial coordinate.

To complete the description of the dynamics of the system, Eqs. 4 and 5 must be complemented by boundary conditions for the velocity on the conduit walls, $V_z(r=R,t)$. These boundary conditions are controlled by the kinetics of the first-order phase transition driven by the value of the shear stress $\overline{\sigma}(t) \equiv \sigma_{rz}(t,R)$ near the wall and are written in a general mixed form (Shore et al., 1997):

$$V_z(R,t) = -R\psi(t) \frac{\partial V_z(r,t)}{\partial r}\Big|_{r=R} \qquad (6)$$

The quantity $R\psi(t)$ is usually called a 'slipping length'. Its value shows at what distance inside the wall the linearly extrapolated velocity becomes zero. For $\psi(t) = 0$ the boundary conditions for the velocity are 'stick', i.e. $V_z(R,t) = 0$; for $\psi(t) > 0$ the boundary layers of the UP 'slip' along the walls of the cylinder with some finite velocity, $V_z(R,t) > 0$.

The time evolution of the dimensionless slipping length $\psi(t)$ is determined from the time-dependent Ginzburg–Landau equation, which is the

most simple description of relaxation of a system with a first-order phase transition:

$$\tau_{GL}\frac{d\psi}{dt} = -\frac{dF}{d\psi} \qquad (7)$$

where Ginzburg–Landau τ_{GL} sets a phase transition timescale. Qualitatively, Eq. 7 shows how a system with the first-order phase transition evolves from an unstable to the stable or a metastable phase, which correspond to a minimum of the free energy F. The rate of evolution depends on the local steepness of the free energy well $dF/d\psi$ and the timescale τ_{GL}. The free energy $F(\psi)$ is a usual double-well potential with a tilt depending on the value of the shear stress $\overline{\sigma}(t)$ on the boundary of the UP. Since the exact form of the potential wells plays very little role in the dynamics of the system, we choose for $F(\psi)$ a double-parabola potential as the most simple suitable form of a double-well potential with fixed positions of both minima, $\psi = 0$ (stick) and $\psi = \psi_0$ (slip):

$$F(\psi) = \begin{cases} \psi^2, & \psi < \psi' \\ (\psi - \psi_0)^2 - h, & \psi \ge \psi' \end{cases} \qquad (8)$$

Here h is a tilt parameter; matching point ψ' is determined from continuity requirement for $F(\psi')$, $\psi' = (\psi_0^2 - h)/2\psi_0$. To determine h and to illustrate how Eqs. 7 and 8 work, let us consider a typical stick–slip cycle. We go around a hysteresis curve shown in Fig. 6. When the shear stress $\overline{\sigma}(t)$ is small and growing (line I), the boundary condition is 'stick' and stationary, $\psi = dF/d\psi = 0$. As the shear stress exceeds the critical value σ_{slip}, the double-parabola topples, $\psi = 0$ seizes to be even a local maximum of $F(\psi)$, and $\psi(t)$ starts moving towards ψ_0 with the rate $\sim 2\psi_0/\tau_{GL}$ (line II). After ψ reaches ψ_0, the boundary condition becomes 'slip' and stationary again, and the shear stress starts decaying (line III). After $\overline{\sigma}(t)$ drops below σ_{stick}, the double-parabola topples in the other way, this time $\psi = \psi_0$ seizes to be even a local maximum of $F(\psi)$, and ψ relaxes to 0 (line IV). The state I corresponds to the dormant period, the state III corresponds to the explosion without intermediate sticking; the transition intervals II, IV are usually very short ($\sim \tau_{GL}$). For the double parabola $F(\psi)$ to topple when the shear stress $\overline{\sigma}$ attains the slip and stick values, σ_{slip}
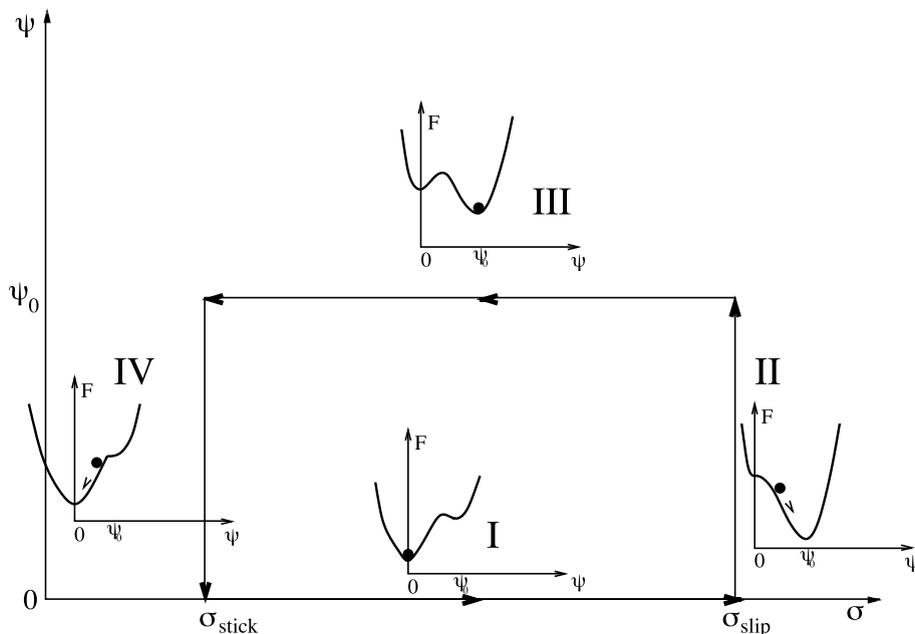

Fig. 6. Hysteresis curve I–II–III–IV for the stick–slip and the slip–stick transitions. Inserts show typical sketches of $F(\psi)$ for all branches of the curve.

and σ_{stick}, the free energy tilt parameter h must be linearly related to $\overline{\sigma}$:

$$h = \psi_0^2 \left[\frac{2\overline{\sigma}}{\sigma_{\text{slip}} - \sigma_{\text{stick}}} - \frac{\sigma_{\text{slip}} + \sigma_{\text{stick}}}{\sigma_{\text{slip}} - \sigma_{\text{stick}}} \right] \qquad (9)$$

Similar to Eq. 4 for the velocity, in the framework of the Maxwell model the shear stress $\overline{\sigma}(t)$ is expressed as a convolution of a shear rate $\partial V_z(r,t')/\partial r$ with an exponentially decaying memory function $\exp\left(-(t-t')/\tau_{\text{m}}\right)$:

$$\overline{\sigma}(t) = \frac{\eta}{\tau_{\text{m}}} \int^t \exp\left(-\frac{t-t'}{\tau_{\text{m}}}\right) \frac{\partial V_z(r,t')}{\partial r}\Big|_{r=R} \, dt' \qquad (10)$$

Eqs. 4–10 completely define the dynamics of our model. A very similar set of equations was derived by Shore et al. (1997) for the physically equivalent model of polymer extrusion. Because of the strong non-linearity of Eq. 7, a complete analytic solution of these equations is impossible. We refer readers to Shore et al., 1997, for a detailed description of a linear stability analysis of this system. Contrary to a stable flow, a dynamical regime corresponding to volcanic activity is strongly unstable and non-linear. However, large separation of characteristic timescales allows us to give analytic estimates of both short (~ 1 s) and long (3–30 min) periods of the temporal behavior of the model.

Let us first look at the shortest timescale which corresponds to small oscillations of the UP when it slips along the conduit walls without intermediate sticking. For this timescale the pressure changes are negligible. Dynamics of the UP is described by Eq. 4 with $P_0 = $ constant and is equivalent to the damped oscillation of an elastic circle membrane with the mixed boundary conditions (Eq. 6). Generally, the lowest harmonic is excited the most, so we seek a solution in a form:

$$V_z(r,t) = V_0 \, e^{-i\omega t} \, J_0\left(\frac{r}{R}\lambda\right) \qquad (11)$$

where λ is a number of order one which depends on the slipping length ψ via the equation $J_0(\lambda) = J_1(\lambda)\lambda\psi$. Here J_0 and J_1 are the zero- and first-order Bessel functions. After plugging Eq. 11 into Eq. 4 and disregarding the constant pressure term, we obtain the following dispersion relation for the oscillating UP:

$$\omega = \frac{-i \pm \sqrt{4\dfrac{\lambda^2 \eta \tau_{\text{m}}}{R^2 \rho} - 1}}{2\tau_{\text{m}}} \qquad (12)$$

This yields for a period T_{osc} of not too overdamped UP oscillations ($T_{\text{osc}} \gg \tau_{\text{m}}$):

$$T_{\text{osc}} \approx \frac{2\pi R}{\lambda} \sqrt{\frac{\rho \tau_{\text{m}}}{\eta}} \qquad (13)$$

Taking into account a commonly used relation between the Maxwell time τ_{m}, viscosity η, and shear modulus G, $\tau_{\text{m}} \approx \eta/G$ (see, for example, Webb, 1997), we observe that Eq. 13 reduces to a usual expression for a period of small free oscillations of an elastic membrane:

$$T_{\text{osc}} \approx \frac{2\pi R}{\lambda} \sqrt{\frac{\rho}{G}} \qquad (14)$$

This gives the estimate for the tremble (or chugging) period. Now we go to much longer timescales, $T \gg \{T_{\text{osc}}, \tau_{\text{m}}\}$ and look first at the steady state UP boundary shear stress:

$$\overline{\sigma} = \frac{\partial V_z(r)}{\partial r}\Big|_{r=R}$$

Since this timescale is much greater than the elastic memory time τ_{m}, the viscoelastic term in Eq. 4 is relaxed to a usual viscous term, $\eta \Delta_r V_z(r,t)$. For a steady state, the average over the conduit cross-section velocity $V(t)$ must be equal to V_0. Solving the Navier–Stokes equation for a steady laminar flow with viscosity η in the channel of radius R with the velocity V_0 and the slipping length ψ, we obtain $\overline{\sigma}$ for the shear stress near the wall:

$$\overline{\sigma} = \frac{4V_0\eta}{R} \frac{1}{1 + 4\psi} \qquad (15)$$

It immediately follows that in order for stick–slip repeating cycles to happen, the 'stick' steady state shear stress ($\overline{\sigma}$ for $\psi = 0$) should be greater than σ_{slip} and 'slip' steady state shear stress ($\overline{\sigma}$ for $\psi = \psi_0$) should be less than σ_{stick}. These conditions imply that for the feeding velocity V_0:

$$\frac{\sigma_{\text{slip}} R}{4\eta} < V_0 < \frac{\sigma_{\text{stick}} R (1 + 4\psi_0)}{4\eta} \qquad (16)$$

Besides the steady state properties, we can also

evaluate characteristic times between the stick–slip and the slip–stick phase transitions, i.e. duration of the dormant and the explosive periods. Assuming that these times are much longer than both T_{osc} and τ_m, we again disregard all memory effects in the viscous term in Eq. 4 and consider the flow inertialess by omitting the left-hand-side term $\partial V_z(r,t)/\partial t$. After averaging the remaining part of Eq. 4 over the cross-section of the flow and plugging it in Eq. 5, we obtain for an arbitrary slipping length ψ:

$$\int^t \frac{V_0 - V(t')}{\beta L l} dt' - \frac{8\eta V(t)}{R^2(1+4\psi)} = 0 \qquad (17)$$

Combining the solution of this equation:

$$V(t) = V_0 + C\, e^{-t/t_0}, \; t_0 \equiv \frac{8\eta\beta L l}{R^2(1+4\psi)} \qquad (18)$$

with expressions for stick and slip velocity that follow from Eq. 15, we obtain for dormant (T_d) and explosive (T_e) times:

$$T_d = \frac{8\eta\beta L l}{R^2} \ln \frac{4\eta V_0 - \sigma_{stick} R}{4\eta V_0 - \sigma_{slip} R} \qquad (19)$$

$$T_e = \frac{8\eta\beta L l}{R^2(1+4\psi_0)} \ln \frac{\sigma_{slip}R(1+4\psi_0) - 4\eta V_0}{\sigma_{stick}R(1+4\psi_0) - 4\eta V_0} \qquad (20)$$

Together with Eq. 14 for the tremble period, these expressions give analytic estimates for all important timescales of eruption.

6. Numerical results

To check our analytical predictions and get an overall view of the system dynamics, we solved Eqs. 4–10 numerically. We used a simple Eulerian finite-difference scheme with a uniform radial grid of 50–100 points. All the integrals are approximated by a trapezoid formula. Given that the time step is sufficiently small to avoid von Neumann-type instabilities, this simple difference scheme proved to be sufficiently robust.

We chose the numerical parameters to be in general accordance with the literature (Murase and McBirney, 1973; Hess, 1989; Borgia and Linneman, 1990; Griffiths and Fink, 1993; Bagdassarov et al., 1994; Webb, 1997; Bagdassarov and

Dorfman, 1998) and with our estimate (Eq. 16) to ensure the stick–slip motion pattern. Generally, there is at least an order of magnitude uncertainty in the numerical values of the parameters; hence we do not attempt to prove that we are able to predict the observed time periods (which themselves vary a lot in the course of an eruption) with an exceptional precision. Rather, we select the values of parameters in a reasonably acceptable range to check if the analytic estimates (14, 19, 20) are confirmed by the numerical solution which produces T_{osc}, T_d, and T_e close to the average observed timescales.

The following values were used:
Density $\rho = 2400$ kg/m^3
Dynamic viscosity $\eta = 10^9$ Pa s
Conduit radius $R = 50$ m
UP length $l = 100$ m
LP length $L = 5$ km
Compressibility $\beta = 4 \times 10^{-10}$ Pa^{-1}
Maxwell time $\tau_m = 0.4$ s
Ginzburg–Landau time $\tau_{GL} = 10^{-3}$ s
Average velocity $V_0 = 2 \times 10^{-3}$ m/s
Slipping shear stress $\sigma_{slip} = 10^5$ Pa
Sticking shear stress $\sigma_{stick} = 3 \times 10^4$ Pa
Dimensionless slipping length $\psi_0 = 10$

With this choice of numerical parameters a no-stick explosion takes place, during which the UP moves along the walls of the conduit with the constant slipping length ψR until it finally sticks to the wall at the end of the explosion. For such explosions a choice of phase transition time τ_{GL} does not affect the dynamics, given that it is shorter than explosion time, $\tau_{GL} \ll T_e$. On the other hand, for numerical stability the phase transition time τ_{GL} should be not less than several time steps, hence we chose $\tau_{GL} = 10^{-3}$ s as indicated above.

Plots of averaged over cross-section velocity $V(t)$ and pressure gradient vs. time are presented in Fig. 7. The simulation results for dormant and explosion times, as well as for short-term oscillation period, $T_d^s \approx 530$ s, $T_e^s \approx 21$ s, $T_{osc}^s \approx 0.69$ s are in good agreement with our simple analytical estimates, $T_d = 497$ s, $T_e = 20$ s, and $T_{osc} = 0.69$ s. To calculate T_{osc} we have to solve the equation $J_0(\lambda) = J_1(\lambda)\lambda\psi$, which for $\psi = 10$ yields $\lambda \approx 0.43$. For the stick boundary conditions ($\psi = 0$),
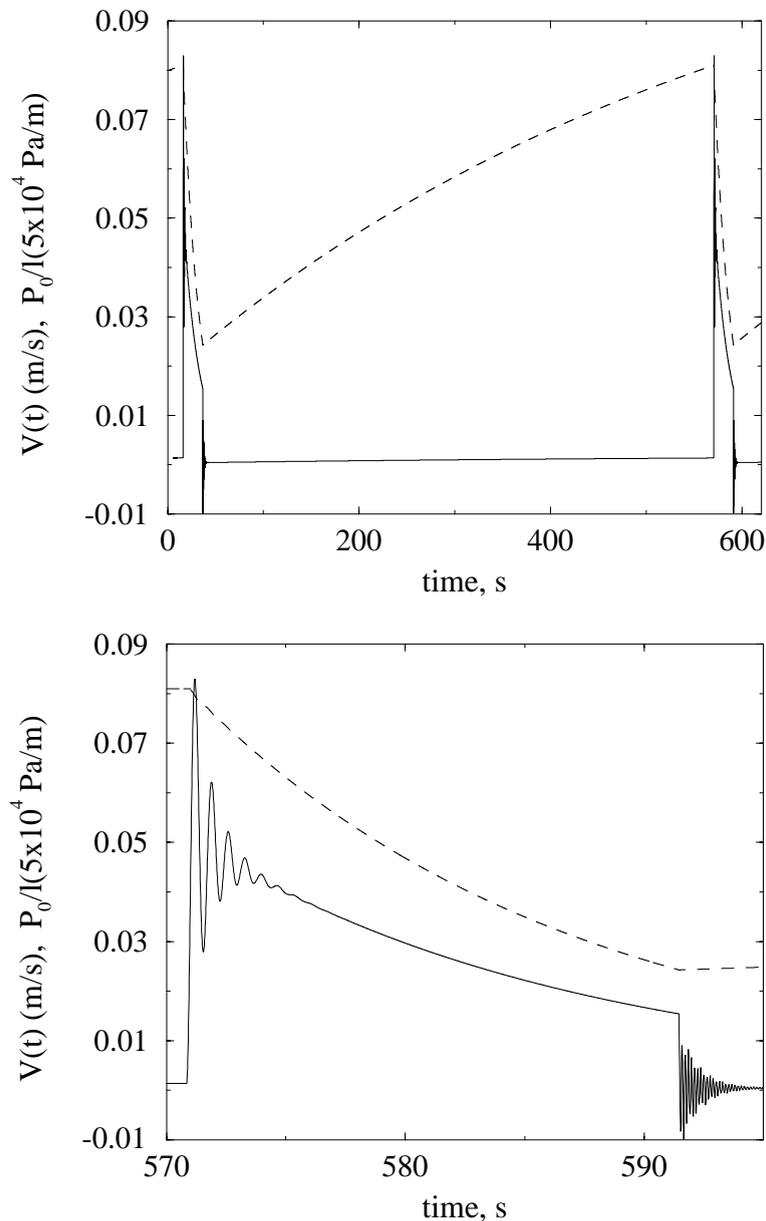
Fig. 7. Time dependence of the spatially averaged UP velocity (solid line) and the rescaled pressure gradient (in 5×10^4 Pa/m, dashed line).

$\lambda \approx 2.3$; which gives for the period of oscillations at the end of explosion cycle when UP is about to stick to the walls $T_{osc}' \approx 0.13$, which is again in very good agreement with the simulation data. Another possible scenario for an eruption is that during an explosion cycle the UP sticks to the walls numerous times. It happens when the shear stress at the wall, modulated by the free membrane-like oscillations of the UP, drops below the sticking value σ_{stick}, and the slip–stick phase transition is sufficiently fast, $\tau_{GL} \ll T_{osc}$. To simulate this regime, we increase the value of σ_{stick}
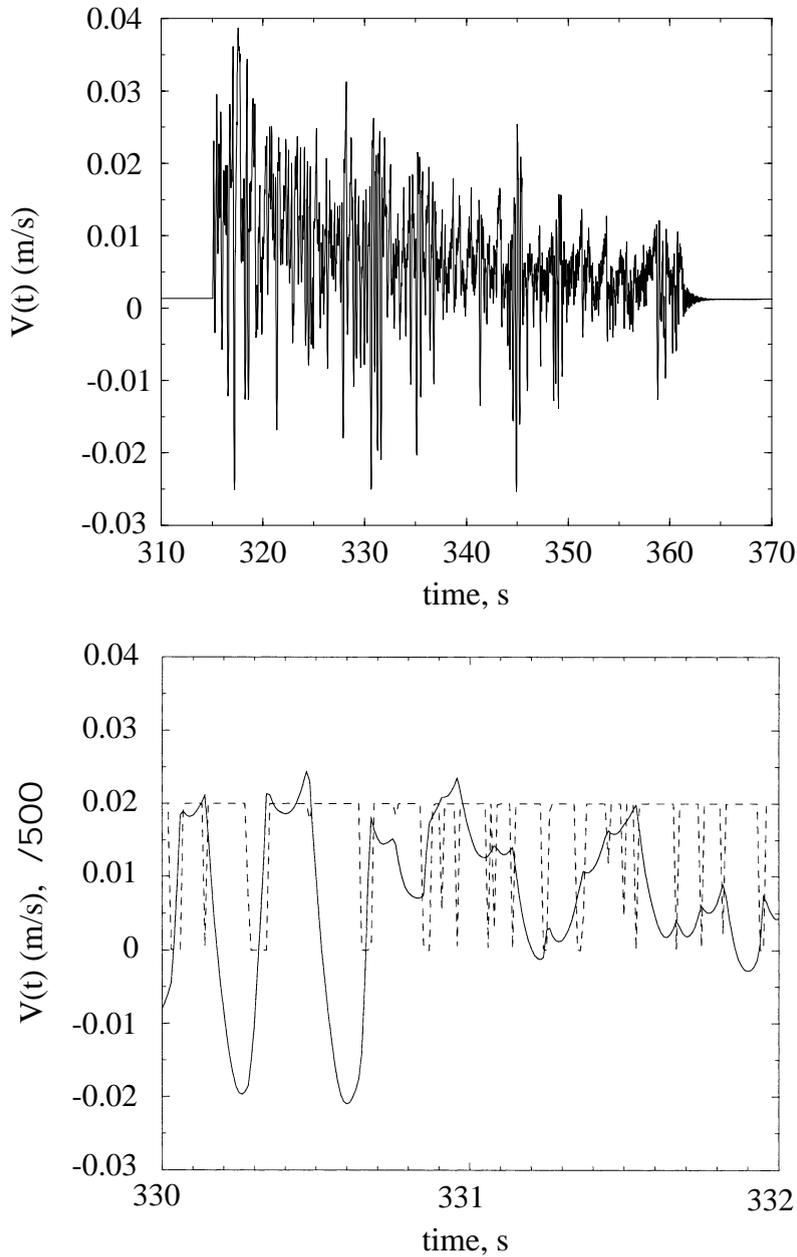
Fig. 8. Time dependence of the spatially averaged UP velocity $V(t)$ (solid line) and the rescaled dimensionless slipping length $\psi(t)/500$ (dashed line).

from 3×10^4 to 8.5×10^4 Pa and keep all other parameters constant. The long-time dynamics, characterized by the times T_e and T_d only slightly changes since both of these times depend on σ_{stick} only logarithmically. However, short-time dynam-ics, previously described by decaying free oscilla-tions with a period T_{osc}, changes radically and becomes chaotic (Fig. 8).

A typical time separation between consecutive velocity maxima (≈ 0.3 s for the first three max-

ima in the bottom part of Fig. 8) becomes somewhat smaller than the free oscillation period $T_{osc} \approx 0.7$. Qualitatively, it happens when during an oscillation the velocity increases so that shear stress drops below σ_{stick}, a sticking occurs that results in a rapid decrease of velocity, so the oscillation is 'truncated' before it reaches its maximum. Another distinct feature of this regime is that the short-time chaotic modulation of the UP velocity continues through the whole explosion phase, while in the non-sticking regime, the oscillations decay after a few periods.

7. Discussion

In the previous sections we derived analytic expressions for all characteristic timescales of the eruption dynamics: short timescale or the period of trembling T_{osc}, dormant T_d and explosive T_e times. We checked our analytic expressions by performing numerical simulations using the rheological and geological parameters that fit reasonably well into their allowed ranges known from the literature and give rise to results that are close to the observed seismic and acoustic signals (Figs. 4, 7 and 8). It was found that the analytic estimates for the timescales are well confirmed by the simulation results. Hence in order to study the dependence of the eruption timescales on the magma and volcano parameters, instead of running computer simulations one can use simple expressions (Eqs. 14, 19 and 20). Among the parameters of the model which enter (Eqs. 14, 19 and 20), the UP length l and the slipping length ψ_0 cannot be directly deduced from the literature or the results of geological studies. Yet the complete knowledge of viscosity profile along the magma conduit can in principle allow one to estimate l. Similarly, laboratory experiments on stick–slip transitions can provide information on the slipping length ψ_0 and the characteristic stick–slip or slip–stick transition time τ_{GL}. Note that τ_{GL} does not enter any of the expressions (Eqs. 14, 19 and 20). It indicates that this time is irrelevant to the general dynamics of the system, given that it is shorter than the shortest important timescale, T_{osc} (which is usually fulfilled by a large margin).

In other words, one can consider these phase transitions instantaneous without a noticeable effect on the results. In the present work, our choice of ψ_0 and τ_{GL} was based on a common sense and the values used in the polymer extrusion literature (Shore et al., 1997). The feeding velocity restriction (Eq. 16) is essential for the explosion–dormant periodic regime of eruption. This condition is somewhat similar to the condition of hysteresis derived by Denlinger and Hoblitt (1999). If the condition (Eq. 16) is satisfied, the dormant and explosive times are given by Eqs. 19 and 20. Taking into account the viscosity of the LP will increase the effective viscosity of the UP η and therefore, increase both of these times. The period of chugging T_{osc} is well estimated by Eq. 14 for both 'sticking' (Fig. 7) and 'non-sticking' (Fig. 8) scenarios. We have not presented a criteria to distinguish which of these scenarios takes place for a given set of parameters. Yet such a criteria would have been of a little value, as the sticking on each cycle of chugging is very short-lived and therefore more sensitive to the UP non-uniformities than the long-term sticking for a dormant period. The fact that chugging is present only during some explosions reveals that its excitation requires special conditions in the conduit; the interaction of moving magma with the conduit walls probably playing the most important role.

Our model contains several rather strong idealizations, such as splitting the magma column into two vertically uniform parts, neglecting viscosity of the lower part and compressibility of the upper part, assuming cylindrical symmetry, and postulating a constant support of magma from the magma chamber. One can take into account some of these neglected effects by creating a more elaborated model and studying it numerically; yet without these simplifications the derivations of Eqs. 14, 19 and 20 would be impossible. Given that the rheological parameters for magma in the conduit and conduit geometry are usually known not better than with an order of magnitude precision, the results of such pure numerical simulation would be of little value, as it is virtually impossible to study the model numerically for all admissible parameters.

Our main goal in this publication was to ex-

plore a physical mechanism responsible for the double-periodic volcanic activity; yet nothing has been said about a generation of seismic and acoustic waves themselves. The oscillating UP and related pressure oscillations in the LP can cause seismic waves either directly or act as a 'pacemaker' for other processes. These processes can include a stimulated emission of gases either through creation and change of geometry of cracks in the UP or via degassing of magma under action of standing and running compression waves. Some seismic observations (Chouet et al., 1999) suggest that the source of the observed long-period signals corresponding to chugging and even whole explosions is sequential pressurization–depressurization of the conduit due to eruptive mass withdrawal and replenishment. Since these mechanisms have a strongly non-linear character, their coupling to the UP oscillation can modify the oscillation period and decay patterns. We leave consideration of these phenomena for future study.

8. Conclusion

As a result of the visual, seismic, and acoustic observations at Karymsky volcano, two scales of temporal periodicity were observed in the eruptive dynamics. First, the repetitive explosions which produced the ash and gas clouds and volcanic bombs in 3–30-min intervals, and secondly, the periodic modulation of eruptive activity (chugging) with a typical timescale of order 1 s. The existence of these two scales of temporal periodicity are not limited to the 1996–2000 eruption of Karymsky volcano, similar timescales were observed during previous Karymsky eruptions and on other andesite volcanoes in the world.

A model of the motion of the magma column was suggested that accounts for both timescales in the eruption of Karymsky and other similar andesite Strombolian-type volcanoes. The model is based on the hydrodynamical description of the viscoelastic lava flow and Ginzburg–Landau theory accounting for stick–slip transitions in magma near the conduit wall. Low- and high-frequency periodicity is caused by two distinct ways

of accumulation of the elastic energy. The viscoelastic properties of the magma in the upper part of the conduit causes the high-frequency tremor, while the bulk compressibility of the magma explains the low-frequency cycles. The shear-stress-dependent stick–slip phase transition of the magma in the upper part of the conduit introduces the hysteresis into the dynamics of the magma column motion and explains the non-harmonic nature of the oscillations and long dormant periods in the eruption dynamics. Physical simplicity of the model allowed to obtain analytic estimates for the long and short periods of the explosive activity.

Acknowledgements

References

Bagdassarov, N.S., Dingwell, D.B., Webb, S.L., 1994. Viscoelasticity of crystal- and bubble-bearing rhyolite melts. Phys. Earth Planet. Inter. 83, 83–99.

Bagdassarov, N., Dorfman, A., 1998. Viscoelastic behavior of partially molten granites. Tectonophysics 290, 27–45.

Benoit, J.P., McNutt, S.R., 1997. New constraints on source ofvolcanic tremor at Arsenal Volcano, Costa Rica, using broadbandseismic data. Geophys. Res. Lett. 24, 449–452.

Bird, R.B., Armstrong, R.C., Hassager, O., 1987. Dynamics of Polymeric Liquids, Vol.1: Fluid Mechanics. Wiley, New York.

Borgia, A. and Linneman, S.R., 1990. On the mechanism of

lava flow emplacement and volano growth: Arenal, Costa Rica. In: Fink, J.H. (Ed.), Lava Flows and Domes. Springer.

Chouet, B., Saccorotti, G., Dawson, Ph., Martini, M., Scarpa, R., De Luca, G., Milana, G., Cattaneo, M., 1999. Broadband measurements of the sources of explosions at Stromboli Volcano, Italy. Geophys. Res. Lett. 26, 1937–1940.

Denlinger, R.P., Hoblitt, R.P., 1999. Cyclic eruptive behavior of silicic volcanoes. Geology 27, 459–462.

Farberov, A.I., Storcheus, A.B., Pribulov, E.S., 1983. Studies of weak seismicity of Karymsky volcano, August 1978 (in Russian). Vulkanol. Seismol. 3, 78–89.

Fedotov, S.A., Ozerov, A.Yu., Magus'kin, M.A., Ivanov, V.V., Karpov, G.A., Leonov, V.L., Dvigalo, V.N., Grib, E.N., Andreev, V.I., Lupikina, E.G., Ovsyannikov, A.A., Budnikov, V.A., Bahtiarov, V.F., Levin, V.E., 2001. 1996–2000 Karymksy eruption and corresponding seismic, geodynamic, and postvulcanic processes and their impact on the environment. In: Global'nuje Uzmenenija Ukrujayushei Uredyu, in press (in Russian).

Griffiths, R.W., Fink, J.H., 1993. Effects of surface cooling on the spreading of lava flows and domes. J. Fluid Mech. 252, 667–702.

Hess, P.S., 1989. Origins of Igneous Rocks. Harvard Univ. Press, Cambridge.

Hrenov, A.P., Dubik, Yu.M., Ivanov, B.V., 1982. Eruptions of Karymsky volcano in 1970–1980 (in Russian). Vulkanol. Seismol. 3, 29–47.

Jaupart, C., Vergniolle, S., 1989. The generation and collapse of a foam layer at the roof of a basaltic magma chamber. J. Fluid Mech. 203, 347–380.

Johnson, J.B., 2000. Interpretation of Unfrasound Generated by Erupting Volcanoes and Seismological Energy Partitioning during Strombolian Explosions. PhD Thesis, University of Washington, Seattle.

Johnson, J.B., Lees, J.M., 2000. Plugs and Chugs – Strombolian activity at Karymsky, Russia, and Sangay, Ecuador. J. Volcanic. Geotherm. Res. 101, 67–82.

Johnson, J.B., Lees, J.M., Gordeev, E.I., 1998. Degassing explosions at Karymsky volcano, Kamchatka. Geophys. Res. Lett. 25, 3999–4000.

Julian, B.R., 1994. Volcanic tremor: Nonlinear excitation by fluid flow. J. Geophys. Res. 99, 11859–11877.

Lees, J.M., Bolton, E.M., 1998. Pressure cookers as volcano analogues. EOS, Trans. Am. Geophys. Union 79(45), Fall Meeting Suppl., F620.

Magus'kin, M.A., Enman, V.B., Seleznev, B.V., Shkred, V.I., 1982. Peculiarities of the Earth core displacement on Karymskyvolcano in 1970-1981 from geodesical and photogrammetric data (in Russian). Vulkanol. Seismol. 4, 49–64.

Manga, M., 1996. Waves of bubbles in basaltic magmas and lavas. J. Geophys. Res. 101, 17457–17465.

Murase, T., McBirney, A.R., 1973. Properties of some common igneous rocks and their melts at high temperatures. Geol. Soc. Am. Bull. 84, 3563–3592.

Ozerov, A.Yu., 1997. Dynamics of the 1996 Karymsky volcano eruption and the composition of its products (in Russian). Vestnik DVO RAN 4, 86–93.

Persson, B.N.J., 1999. Sliding Friction. Springer, chapter 8.

Shirokov, V.A., Ivanov, V.V., Stepanov, V.V., 1988. On the deep structure of Karymksy volcano and peculiaritiesof its seismicity: local seismic network data (in Russian). Vulkanol. Seismol. 3, 71–80.

Shore, J.D., Ronis, D., Piche, L., Grant, M., 1997. Theory of melt instabilities in the capillary flow of polymer melts. Phys. Rev. E 55, 2976–2992.

Tokarev, P.I., Firstov, P.P., 1967. Seismological studies of Karymsky volcano (in Russian). Bulluten' Vulkanol. Stanciy 43, 9–22.

Webb, S., 1997. Silicate melts: Relaxation, Rheology, and the Glass transition. Rev. Geophys. 35, 191–218.

Zubin, M.I., Ivanov, B.V., Shteinberg, G.S., 1971. Structure of Karymskyvolcano, Kamchatka, and some aspects of caldera genesis (in Russian). Geol. Geofiz. 1, 73–81.